Astron. Astrophys. 343, 899–903 (1999)

ASTRONOMY AND ASTROPHYSICS

Hubble Deep Field guide star photometry⋆

K. Zwintz[1], **R. Kuschnig**[1], **W.W. Weiss**[1], **R.O. Gray**[2], **and H. Jenkner**[3,4]

[1] Institute for Astronomy, University of Vienna, Türkenschanzstrasse 17, A-1180 Vienna, Austria (last_name@galileo.astro.univie.ac.at)
[2] Department of Physics and Astronomy, Appalachian State University, Boone, NC 28608, USA (grayro@conrad.appstate.edu)
[3] Space Telescope Science Institute, 3700 San Martin Drive, Baltimore, MD 21218, USA (jenkner@stsci.edu)
[4] On assignment from the Astrophysics Division, Space Science Department, European Space Agency (ESA)

Received 20 July 1998 / Accepted 24 December 1998

Abstract. Since the advent of asteroseismology as a promising innovative tool for investigating internal stellar structure, numerous attempts to detect solar type oscillations in distant stars have been conducted. The three Fine Guidance Sensors of the Hubble Space Telescope can contribute to asteroseismology, but only after the data have been corrected for systematic effects, the South Atlantic Anomaly and terrestrial stray light being the most important. We have applied these corrections and obtained essentially photon noise-limited photometry for two guide stars used during the Hubble Deep Field program.

Ground-based spectral classification has revealed that the brighter of the two guide stars is a solar-type star with a spectral type of G2mG0IV. Fine Guidance Sensor photometry for this star gives a noise level in the amplitude spectrum of only 23 ppm, which makes it a good candidate for detecting stochastically driven oscillations. We compare our result with theoretical predictions.

The second guide star was classified as K1V and therefore is not a candidate for solar type oscillations.

Key words: techniques: photometric – stars: fundamental parameters – stars: individual: GS 0416200054 – stars: individual: GS 0416200075 – stars: oscillations

1. Introduction

With the success of helioseismology in testing solar models and in investigating hitherto speculative issues, such as internal solar rotation, observational evidence for stochastically driven oscillation in stars other than our Sun has gained increasing interest. So far, results have been disappointing (Kjeldsen & Bedding 1995) and controversial (for example: α Cen, Procyon, η Boo).

The question of how solar luminosity variations scale to stars with different $T_{\rm eff}$ and $\log g$ is important when selecting target stars for expensive observing programs and it touches on theoretical areas, such as convection, that are only poorly understood. The most recent investigation of this scaling problem (Houdek 1997) predicts luminosity amplitudes of up to 80 ppm for stars evolved from the ZAMS and close to the cool border of the classical instability strip.

Low-noise photometric time series are needed to detect the largest amplitude frequencies and even more so to determine the characteristic frequency spacings which are important diagnostic tools in asteroseismology. Space-borne experiments, taking advantage of the lack of atmospheric noise, can provide such high quality data. After two ESA Phase-A studies (PRISMA and STARS), the CNES-lead experiment COROT is an approved space experiment devoted to asteroseismology (and the detection of exoplanets), after its smaller precursor, EVRIS, was a victim of the MARS-96 disaster. Other similar projects, such as MONS (Denmark) and MOST (Canada), hopefully will receive funding.

The High Speed Photometer of the Hubble Space Telescope (HST) could have been used to detect solar-type pulsation in stars, but not surprisingly, the large amount of HST time needed for the project to observe even very bright stars has not been granted. However, HST Fine Guidance Sensors (FGS) can contribute to asteroseismology of solar type stars (Kuschnig et al. 1997, referenced in the following as Paper I). To reduce the enormous amount of photometric data points we average the counts typically over 10 sec. As only half of the actually executed FGS integrations (40 samples per second with 25 msec integration time each) are recorded in the telemetry stream which we are forced to use, every other sample is lost for our analysis and consequently the associated S/N ratio is that one would get from a telescope with a collecting area equivalent to a 1.7m primary mirror.

A special observing program was performed in December 1995 with the HST called the "Hubble Deep Field" (HDF) program. A region in the Northern Continuous Viewing Zone was observed for ten consecutive days. This field is located high above the galactic plane at a right ascension of $12^{\rm h}36^{\rm m}49\overset{\rm s}{.}4$ and a declination of $+62^\circ12'58''$ (J2000.0) and contains no bright stars or other previously studied objects. Therefore it is one of the "darkest" regions in the sky.

Send offprint requests to: Werner W. Weiss (weiss@astro.univie.ac.at)

⋆ Based on observations made with the NASA/ESA *Hubble Space Telescope*, obtained from the data archive at the Space Telescope Science Institute, which is operated by the Association of Universities for Research in Astronomy, Inc., under NASA contract NAS 5-26555.

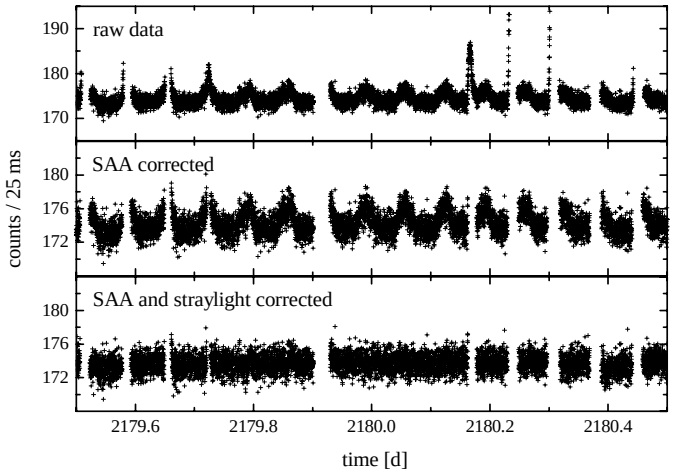

Fig. 1. Light curve of GS-75, third day of the HDF program. *Top:* raw data, *middle:* with correction for the South Atlantic Anomaly (SAA), *bottom:* residual light curve after SAA and stray light correction. Note the different scale for the *top panel*.

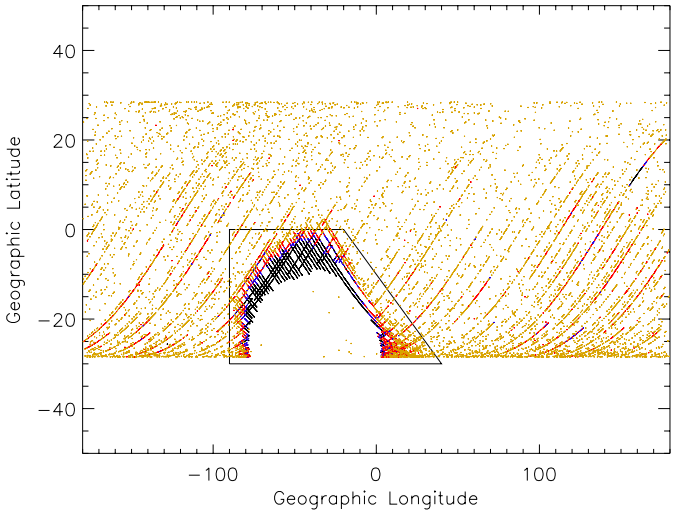

Fig. 2. Map of the intensities measured for GS-75 above a chosen threshold as a function of the geographic position of the HST. An increased density of HST positions (points) for which the FGS countrate exceeded the threshold is clearly visible at the border of the South Atlantic Anomaly. When crossing this anomaly the FGS' were switched off.

Table 1. Position (Epoch J2000) and brightness of the two HDF guide stars (Guide Star Catalog 1992) and their spectral type

GS No.	RA	DEC	m_V	spec. type
0416200054	$12^h35^m10^s$	$+62°16'01''$	11.87	G2mG0 IV
0416200075	$12^h37^m28^s$	$+62°24'51''$	13.05	K1 V

During this period the HST was guided with two of the three Fine Guidance Sensors, and hence photometric time series of the two Guide Stars, GS0416200054 (GS-54, using FGS 3) and GS0416200075 (GS-75, using FGS 2), were obtained. Their position is given in Table 1 as well as their V magnitude. With 10 days of nearly continuous data it is possible to investigate systematic effects occuring in the FGS photometry and to reach a very low noise level in the frequency spectra.

2. Investigation of systematic effects

The FGS photometric data had to be extracted from the Engineering-Subset-Data Files of the HST Data Archive at STScI in Baltimore, Maryland. First, datapoints not obtained in "Fine Lock Mode" of the FGS were eliminated. Second, the measurements were averaged over intervals of 10 seconds.

The resulting "raw" light curve of the third day of GS-75 is shown as a typical example in the top panel of Fig. 1 and the presence of systematic effects is obvious. The intensity modulation has two different characteristics. First, high peaks in the count rates, reaching extreme values, appear periodically but not in each orbit. These "spikes" can be identified as the influences from the South Atlantic Anomaly (SAA). The second type of modulation is characterized by changes synchronous to the HST orbit with a period of 96 minutes. The amplitude of this effect decreased during the HDF program. This effect can be explained by stray light contribution from the Earth.

2.1. South Atlantic Anomaly (SAA)

In the Earth's southern hemisphere, near the east-coast of South America, a distortion of the terrestrial geomagnetic field exists. This region is called the South Atlantic Anomaly and its boundary at an altitude of 500 km ranges from -90 and +40 degrees in geographic longitude and from -50 and 0 degrees in latitude. As the spacecraft is exposed to high energy protons and electrons no astronomical or calibration observations are normally performed during passages through the SAA. However, in the transition zones to the SAA the FGS did measure already increased intensities before the PMTs were switched off. To map the influence of the SAA on the data we calculated the subsatellite position of the HST in geographic coordinates and indicated any positions for which the FGS count rate exceeded a given threshold (Fig. 2). An increase in count rates at the boundaries of the SAA is clearly visible, which is consistent with models in the literature (e.g. Zombeck 1992).

As it was not possible to model reliably the boundary to the SAA we had to remove all "bad" data obtained within a heuristically determined trapezoidal shaped area (Fig. 2) from the photometric time series. The same figure also illustrates that the orbit of the HST approaches the southern auroral zone, as is evident from a slightly increased background level at the most negative latitudes. Furthermore, there is an indication for an area of slightly enhanced radiation just opposite to the SAA. The middle panel of Fig. 1 shows the data corrected for the SAA.

2.2. Contribution of stray light

A residual harmonic variation with the HST orbital period of 96 minutes and with a decreasing amplitude during the ten days remained in the data after the correction for effects due to the

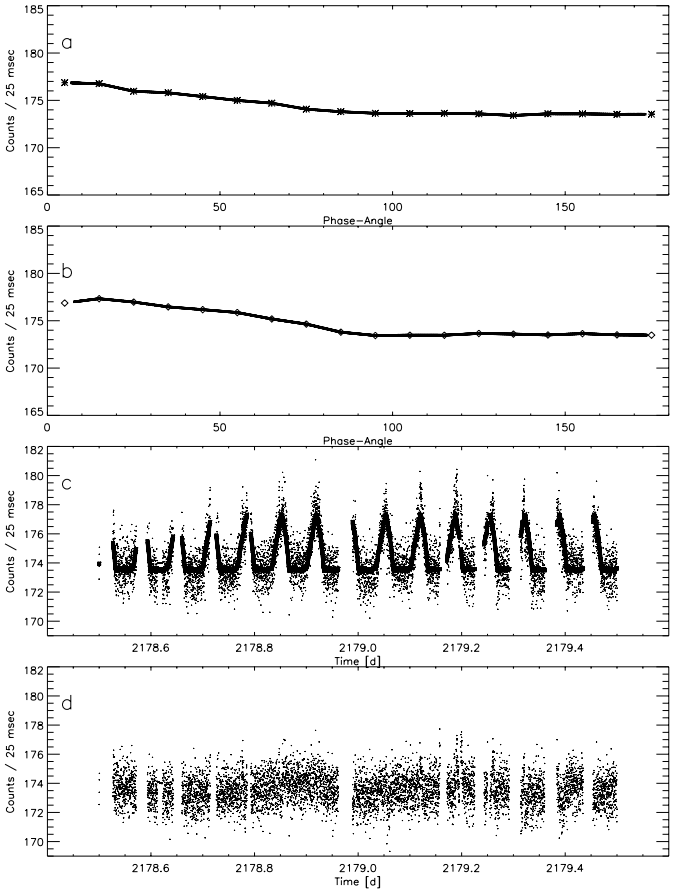

Fig. 3a–d. Stray light Correction for GS-75 and the second day of the HDF program – **a** stray light west, **b** stray light east, **c** uncorrected light curve with superposed stray light contribution computed from linear interpolations between appropriately chosen bins in panel **a** or **b**, respectively, **d** stray light corrected light curve

SAA. This effect can be explained as stray light coming from the illuminated Earth below the spacecraft. The brightness variations are a consequence of the changing aspect of the sunlit Earth relative to the spacecraft. Our result confirms the predictions (Petro 1995) for the contribution of background light in the Hubble Deep Field.

For a fuller analysis, the phase angle ϕ between the Sun and the position of the HST was calculated according to simple spherical trigonometry:

$$\cos\phi = \sin b_{\odot} \cdot \sin b_{HST} + \\ + \cos b_{\odot} \cdot \cos b_{HST} \cdot \cos(l_{HST} - l_{Sun})$$

with b and l the geographic latitude and longitude of the sun and the HST, respectively.

For $\phi = 0°$ the HST is positioned right over the fully illuminated Earth, while at $\phi = 180°$ the HST flies over "mid-night" sites, and the HST crosses the terminator at $\phi = 90°$. Hence, the contribution of scattered light from the Earth increases with decreasing phase angle ϕ. As the orbit inclination of the HST is 28.5° and the orbital precession period is about 56^d, the phase angle usually does not reach the extreme values of 0° and 180°.

To determine the amount of stray light correction, ϕ was binned in intervals of 10° and the count rates were averaged over an observing period of 24^h. A smaller size of the binning interval would potentially allow to better model possible details of the stray light function, but this advantage would be lost by the larger scatter of the average bin values due to less data points per (smaller) bin. Any high frequency pulsation would be smeared out with this procedure. The stray light effect is not symmetric around $\phi = 0°$ (Fig. 3) because of the orientation of the optical axis of the HST. Therefore the stray light correction over the eastern hemisphere is different from the western hemisphere. An example for the procedure is shown in Fig. 1. For a given phase angle the correction was computed from a linear interpolation between appropriately chosen bins.

2.3. Problems with FGS 2

In addition to the contribution of the SAA and the stray light contamination we found an error in the FGS 2 measurements. During an 11^h time interval of the 10 days HDF program the count rates of both PMTs in the FGS 2 Y-axis dropped significantly, but the X-axis channels were not affected. For technical details, the meaning of X- and Y-axes, working principles, etc., see Holfeltz et al. (1995). As we add the counts of all four PMTs to a single photometric data point (see Paper I), the total intensity decreased by about 20%. The electronics of the Y-axis components recovered towards the end of the 11^h period to the count rate observed before the interval. The origin of this effect presently is unknown and data points obtained during this time were excluded from the final analysis. No evidence for a similar behavior was found throughout the whole HDF program in the FGS3 (GS-54) data sets.

3. Fourier analysis

A period search on the "cleaned" datasets (SAA and stray light corrected) was carried out with a standard Fourier technique (Deeming 1975). The resulting amplitude spectra for both stars reveal a number of significant frequencies (see Tables 2 and 3). A signal is considered to be significant, if the amplitude is at least four times larger than the noise level (Paper I). Since stars in the continuous viewing zone were observed, the duty cycle was large and hence the window function of the Fourier transform is clean with very small side lobes.

Two groups of frequencies were determined and heuristically identified. One group, which seems to be related to the orbit ($f_1 - f_8$) and another one, of yet unknown source, which is clearly present in both guide star data sets and hence is probably not intrinsic but of instrumental origin. The orbital modulation which remains after correction for the SAA comes from the residual background modulation (Fig. 2) and the averaging procedure over 24^h when determining the stray light correction.

In the next step the light curves of both guide stars were prewhitened with the frequencies and amplitudes determined with a simultaneous multi-sine fit, as given in Tables 2 and 3. The amplitude spectra of GS-54 and GS-75, cleaned for iden-

Table 2. List of eliminated frequencies for GS-54 (1 d^{-1} = 11.6 μHz).

	Frequency [d^{-1}]	Amplitude [ppm]	Comments
f_1	13.91	129	$f_1 = orbit$
f_2	27.83	109	$2 * f_1$
f_3	41.74	145	$3 * f_1$
f_4	83.48	58	$6 * f_1$
f_5	7.02	96	$1/2 * f_1$
f_6	26.79	134	$f_2 - 1\,d^{-1}$
f_7	28.85	91	$f_2 + 1\,d^{-1}$
f_8	42.79	153	$f_3 + 1\,d^{-1}$
f_9	57.73	91	GS75 & GS54
f_{10}	58.66	65	$f_9 + 1\,d^{-1}$
f_{11}	86.49	80	GS75 & GS54
f_{12}	115.31	96	GS75 & GS54
f_{13}	0.62	120	GS75 & GS54

Table 3. List of eliminated frequencies for GS-75

	Frequency [d^{-1}]	Amplitude [ppm]	Comments
f_1	13.91	495	$f_1 = orbit$
f_2	27.82	294	$2 * f_1$
cd f_3	41.73	317	$3 * f_1$
f_4	69.55	202	$5 * f_1$
f_5	6.94	300	$1/2 * f_1$
f_6	26.82	305	$f_2 - 1\,d^{-1}$
f_7	28.93	184	$f_2 + 1\,d^{-1}$
f_8	42.79	351	$f_3 + 1\,d^{-1}$
f_9	57.70	236	GS75 & GS54
f_{10}	86.55	253	GS75 & GS54
f_{11}	115.44	184	GS75 & GS54
f_{12}	0.61	622	GS75 & GS54

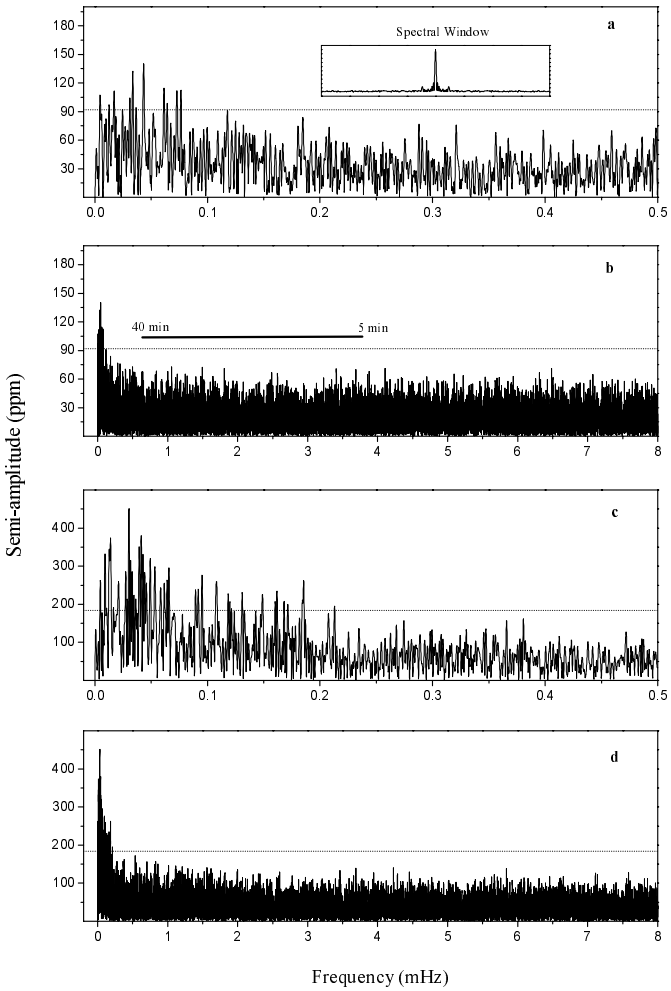

Fig. 4a–d. Amplitude spectra, after removal of identified non-intrinsic variations, for GS-54 (*upper two panels*) and GS-75 (*lower two panels*).

tified non-intrinsic effects, are shown in Fig. 4. In the low frequency domain from 0 to about 0.1 mHz for GS-54 (noise level at 23 ppm) and from 0 to 0.2 mHz for GS-75 (noise level at 47 ppm) numerous peaks can still be found above the 99.9% significance level (dotted lines). Whether these peaks are caused by long term stellar variability or can be interpreted as signal due to granulation similar to our sun, or by complex instrumental effects cannot be decided at this time.

4. Spectral classification

Classification-resolution spectra were obtained for both GS-54 and GS-75 with the Gray/Miller spectrograph on the 0.8 m telescope of Appalachian State University on the morning of Feb 1, 1998. A 600g/mm grating was used with a TI 1024 $\times$ 1024 thinned CCD to give a resolution of 3.6 Å for 2 pixels and a wavelength coverage of 3800–5600 Å. Both spectra have a S/N ~ 100. The spectra were reduced using standard routines under IRAF. The rectified spectra were compared with a library of MK standards obtained with the same system, giving the following classifications: G2mG0IV (GS-54) and K1V (GS-75).

The G2mG0 type indicates that GS-54 is a slightly metal-weak G2 star; it also appears to be slightly evolved. We have attempted to fit a synthetic spectrum (calculated using the spectral synthesis program SPECTRUM - Gray & Corbally (1994), using Kurucz 1993 ATLAS 9 models) to the observed spectrum. Our best fit gives $T_{\rm eff} = 6000\mathrm{K} \pm 140\mathrm{K}$, $\log g = 4.0 \pm 0.25$, $[M/H] = -0.2 \pm 0.2$ assuming $\xi_t = 2.0\,\mathrm{km\,s^{-1}}$ (see Fig. 5).

5. Conclusions

During the Hubble Deep Field program two guide stars were observed continuously with Fine Guidance Sensors 2 and 3 over a period of 10 days. A correction for enhanced background radiation due to the South Atlantic Anomaly and for stray light due to the illuminated Earth beneath HST resulted in photometric time series which are essentially photon noise limited. For frequencies larger than about 0.1 mHz only the two effects mentioned above influence the FGS photometry and the instrument itself proved to be very stable.

The spectral types of the two guide stars were determined to be G2mG0 IV and K1 V and the noise level in the amplitude

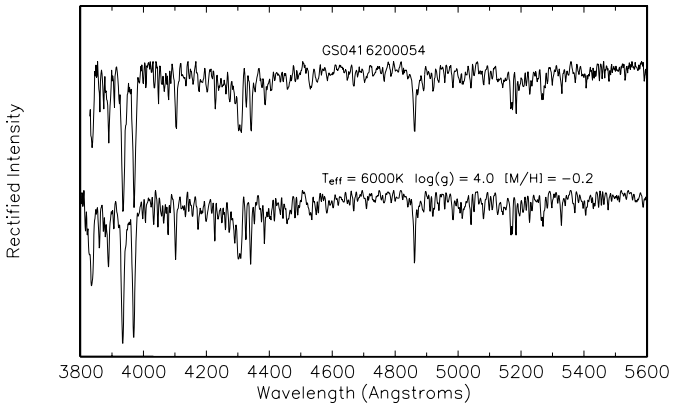

Fig. 5. Spectrum of GS-54 and a synthetic spectrum based on an ATLAS 9 Kurucz model atmosphere.

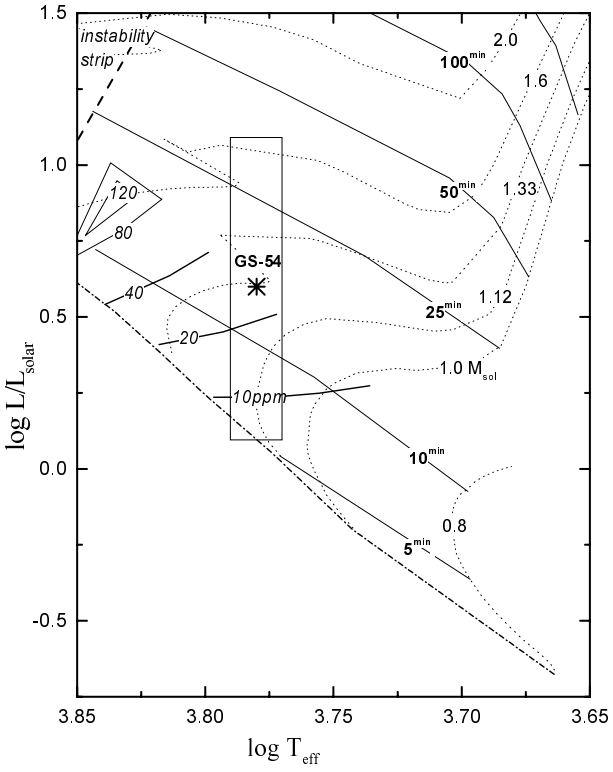

Fig. 6. HR-diagram and evolution tracks (Gimenez 1995) of 1 to 2 solar mass stars. The box centered on GS-54 corresponds to the uncertainties of the respective quantities derived from spectroscopy. The cool observed border of the classical instability strip is given as well as lines of constant estimated luminosity amplitudes (Houdek 1997) and of extrapolated period of maximum pulsation amplitude (Kjeldsen & Bedding 1995).

spectra found to be 23 ppm and 47 ppm, respectively. According to computations of luminosity amplitudes for solar-type pulsation (Houdek 1997), the expected maximum amplitude for the G-type star (GS-54) should be between 10 and up to 80 ppm (Fig. 6) with an estimated period for the maximum amplitude of about 7 to 30 minutes, using the scaling relation of Kjeldsen & Bedding (1995). No increase of amplitudes exceeding the noise level of 23 ppm is present in the frequency range of interest (Fig. 4), what might indicate a possible overestimation of the luminosity variations computed by Houdek, a fact which may be important for planning future ground based observing campaigns as well as for selecting targets for space experiments.

In spite of the lack of an unambiguous pulsation, the data themselves are of extremely high quality, demonstrating the potential of the Hubble Space Telescope Fine Guidance Sensors to provide observations which are well suited for asteroseismic investigations. Considering the importance of a clear detection of solar type pulsation for the first time also in stars other than our Sun, it would be highly desirable to select guide stars accordingly. Slightly evolved bright late F-type stars are prime targets for this project.

Acknowledgements. This work was performed within the working group *Asteroseismology-AMS* and received funding from the Österreichische Nationalbank (project 6713: *Mikrovariabilität von Sternen*), Fonds zur Förderung der wissenschaftlichen Forschung (project *S-7303AST*) and from Digital Equipment Corp. (European External Research Programme, project *STARPULS*). We would like to thank Benoit Pirenne from ST-ECF, ESO Germany, for access to the HST Definitive Ephemeris Files.

References

Guide Star Catalog 1992, Space Telescope Science Institute, CD-ROM
Deeming T.J. 1975, Ap&SS 36, 137
Gimenez A., 1995, A&AS 109, 441
Gray R.O., Corbally C.J., 1994, AJ 107, 742
Holfeltz S.T., Nelan E.P., Taff L.G., Lattanzi M.G., 1995, HST Fine Guidance Sensors Instrument Handbook, Version 5.0. Space Telescope Science Institute
Houdek G., 1997, Pulsation of solar type stars. Thesis University Vienna
Kjeldsen H., Bedding T.R., 1995, A&A 293, 87
Kurucz R.L. 1993, CD-ROM 13, ATLAS 9 Stellar Atmosphere Programs and 2 km s^{-1} Grid (Cambridge: Smithsonian Astrophys. Obs.)
Kuschnig R., Weiss W.W., Gruber R., Bely P.Y., Jenkner H., 1997, A&A 328, 544 (Paper I)
Petro L., 1995, STScI Internal Report, July 6
Williams R.E., Blacker B., Dickinson M., et al., 1996, AJ 112, 1335
Zombeck M.V., 1992, Handbook of Space Astronomy & Astrophysics. 2nd edition, Cambridge Univ. Press, Cambridge